

Photonic Crystal Fiber Interferometric Force Sensor

Joel Villatoro, Vladimir P. Minkovich, *Member, IEEE*, and Joseba Zubia

Abstract—A compellingly simple force sensor based on a photonic crystal fiber (PCF) mode interferometer is presented. A mechanical piece with grooves is used to convert the external force in localized pressure on the sensitive part of the interferometer. The localized pressure on the PCF causes attenuation losses to the interfering modes and makes the interference pattern to shrink. The changes of the interference pattern are quantified by means of Fourier transformation. In the sensing architecture here proposed, temperature or power fluctuations of the light source do not affect the measurement.

Index Terms—Photonic crystal fiber interferometers, optical fiber sensors, mode interferometers, force sensor, pressure sensor.

I. INTRODUCTION

SENSING or monitoring physical parameters with optical fibers has important advantages which include high sensitivity, compactness, and immunity to electromagnetic interference, among others. Force sensing, for example, is important in medical and/or industrial applications as it can provide tactile or touch information. For such applications, force sensors as simple as possible and with miniature size are crucial since they are embedded inside instruments, devices or mechanical pieces.

So far, several approaches had been proposed to sense force with optical fibers. Most of them exploit either fiber Bragg gratings (FBGs) [1]–[4], interferometry [5]–[7] or intensity changes [8]–[10]. The main disadvantages of such sensors are the high cost of FBG interrogators, the intrinsic ambiguity of phase shift measurements, or the dependence to uncontrollable disturbances (e.g. temperature or power fluctuations, attenuation losses, etc.). All these factors limit the applications of current fiber optic force sensors.

In this letter, we report on a force sensor based on a photonic crystal fiber (PCF) mode interferometer which is described in detailed elsewhere [11], [12]. Force on the interferometer is applied with two metal plates, one has a single or two

Manuscript received October 17, 2014; revised January 23, 2015; accepted March 3, 2015. Date of publication March 11, 2015; date of current version May 11, 2015. This work was supported in part by FEDER, the Ministerio de Economía y Competitividad, Spain, under Project TEC2012-37983-C03-01, in part by the Gobierno Vasco/Eusko Jaurlaritza under Project IT664-13 and Project ETORTEK14/13, and in part by the University of the Basque Country, Bilbao, Spain, through Research Program under Grant UFI11/16 and Grant US13/09, and EUSKAMPUS.

J. Villatoro is with the Department of Communications Engineering, Escuela Técnica Superior de Ingeniería de Bilbao, University of the Basque Country, Bilbao 48049, Spain, and also with IKERBASQUE—Basque Foundation for Science, Bilbao 48011, Spain (e-mail: agustinoel.villatoro@ehu.es).

V. P. Minkovich is with the Centro de Investigaciones en Óptica, A.C., León 37150, Mexico (e-mail: vladimir@cio.mx).

J. Zubia is with the Department of Communications Engineering, Escuela Técnica Superior de Ingeniería de Bilbao, University of the Basque Country, Bilbao 48049, Spain (e-mail: joseba.zubia@ehu.es).

Color versions of one or more of the figures in this letter are available online at <http://ieeexplore.ieee.org>.

Digital Object Identifier 10.1109/LPT.2015.2411312

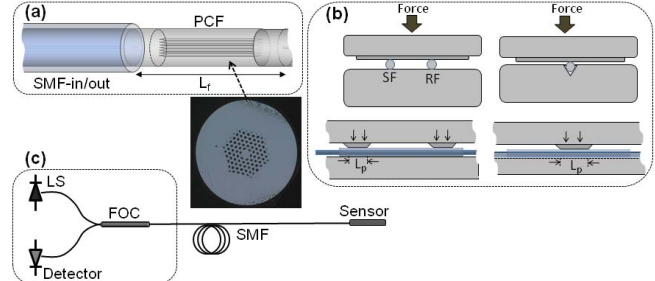


Fig. 1. (a) Drawing of a photonic crystal fiber (PCF) mode interferometer. L_f is the length of PCF. The micrograph shows the cross section of the PCF used in the experiments. (b) Schematic representation of the front and lateral views of two configurations to measure force. SF and RF are, respectively, sensing and reference fiber. L_p is the length of contact on the PCF. (c) The interrogation of the interferometer is carried out with conventional single-mode optical fiber (SMF), a broadband light source (LS), a fiber optic circulator or coupler (FOC), and a detector.

grooves and the other is smooth or has a V-groove to partially embed the PCF, see Fig. 1. In our configuration, the external force on the metal pieces is converted in localized pressure on the sensitive part of interferometer. The localized pressure on the photonic fiber induces stress and strain in the same, as a consequence, the intensity and propagation constant of the interfering modes change [13], [14]. As a result, the interference pattern shifts and shrinks. To convert the changes experienced by the interference pattern into physical force on the device we use Fourier transformation. The advantages of our configuration include simplicity and the fact that temperature or fluctuations of the optical source have no affect on the measurements.

II. DESIGN FOR FORCE SENSING

The PCF mode interferometer used in this letter is compellingly simple; its schematic diagram is shown in Fig. 1. The fabrication of such interferometers has been reported elsewhere [11]. Basically, it consists of fusion splicing a short section of PCF with conventional single mode optical fiber (SMF). In our case, a home-made index-guiding PCF, whose details and modal properties are described in detail in [15], was used. To achieve a mode interferometer the voids of the PCF are completely sealed over a microscopic length during the splicing process. The zones of the PCF with collapsed voids in the PCF-SMF junctions allow the efficient excitation and recombination of two core modes [11].

The transfer function of our interferometers can be expressed by a simple mathematical equation:

$$I = I_1 + I_2 + 2(I_1 I_2)^{1/2} \cos(\Delta\phi), \quad (1)$$

where I_1 and I_2 are the intensities of the two interfering modes and $\Delta\phi$ is the phase difference between the modes.

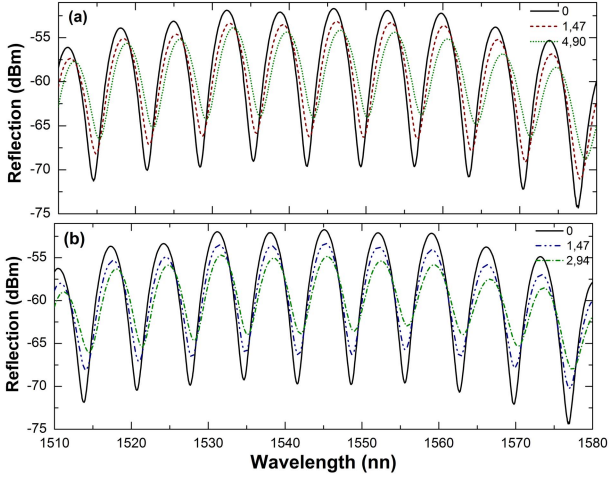


Fig. 2. Reflection spectra at different forces observed in a 3.7 cm-long PCF interferometer when it was pressed with a serrated and flat plate (a) or with a serrated plate and one with a V-groove (b). The separation between the grooves was 7.5 mm and L_p was 1 mm.

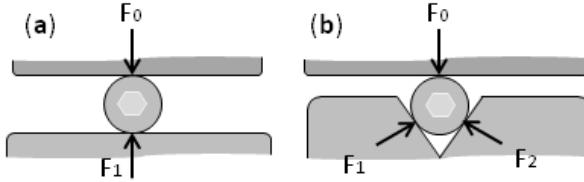


Fig. 3. Schematic representation of two configurations to measure force with a PCF interferometer. (a) The fiber is pressed with flat rigid mechanical pieces. (b) The fiber is pressed into a V groove. The forces acting on the fiber are F_0 , the applied force, F_1 and F_2 , the reaction forces of the mechanical pieces.

The phase difference depends on the length of PCF (L_f), the effective refractive index of the interfering modes, and also on the wavelength of the optical source [11]. Thus, the interference pattern of our PCF mode interferometer exhibits a series of maxima and minima, see Fig. 2. If the interferometer is pressed with serrated pieces or into a V groove then the interference pattern shrinks and shifts remarkably. The shift of the interference pattern or the changes of the fringe contrast (expressed in dB), i.e., the difference between the maxima and minima are easy to detect and quantify [12].

To understand the behavior of our device in Fig. 3 we represent schematically the forces that act on the PCF. An external force (F_0) applied perpendicular to the PCF axis induces stress, defined as F_0/A , where A is the area of the fiber that experiences the external force [13]. As a consequence, the PCF experiences transversal and axial strain [13], [14]. Stress and strain on the PCF modify the intensity and the effective indices of the interfering modes, hence $\Delta\phi$. For this reason the interference pattern shifts and shrinks. To quantify the variation of $\Delta\phi$ and/or I_1 and I_2 as a function of stress and strain one needs to know the elastic moduli of the material that coats and compose the PCF as well as the Poisson ratio and the Young's modulus of such materials. Such calculations are beyond the scope of the present letter. However, it is not difficult to see that if the number of grooves increases then the area of the fiber that experiences the external force

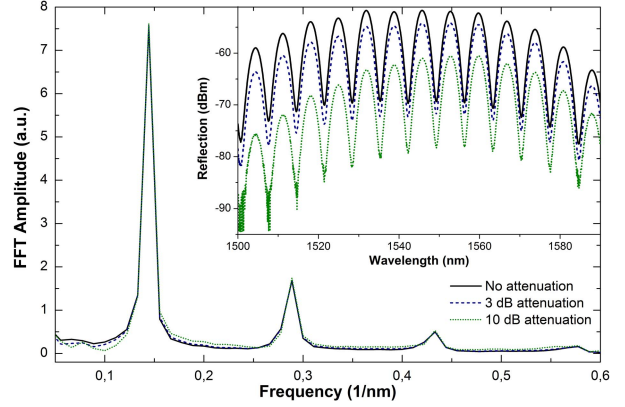


Fig. 4. FFT amplitude versus frequency and reflection spectra (inset) observed in an interferometer without attenuation (solid line), attenuated by 3 dB (dashed line) and 10 dB (dotted line). L_f was 3.7 cm, L_p was 1 mm, and the external force was 0 N.

will increase. As a result, the stress induced on the fiber will diminish.

It is easy to monitor changes of fringe contrast (or visibility) of interference patterns. In fact several research groups have demonstrated sensors based on this concept, see for example, [10], [12], [16]–[18]. However, when one measures the fringe contrast of an interference pattern, the uncertainty increases as the minima approach the floor noise of the detector or spectrum analyzer. This is particularly critical, for example, in a situation of huge attenuation losses. As the light source used to interrogate our sensors is typically a low-power LED, thus, huge losses may be taken into account. Thus, we did some simple experiments to overcome the aforementioned situation that are summarized in Fig. 4. We intentionally induced huge attenuation losses and observed the interference patterns. It can be seen from the figure that the interference pattern preserves its well-defined shape for losses below 10 dB. However, for higher losses the minima of the interference pattern are noisy which introduce errors when one finds the position of the minima; hence the fringe contrast.

As an alternative to measure fringe contrast, and therefore, an external stimulus on the interferometer, here we propose to measure the amplitude of the fast Fourier transform (FFT) of the interference patterns. For example, in Fig. 4 we show the amplitude of the FFT as a function of frequency. The FFT was calculated with the spectra shown in the inset of Fig. 4 which were obtained when the interferometer was subjected to a force of 0 N. It can be noted that the amplitude of the FFT is not affected by a noisy interference pattern which suggests that more accurate sensing can be carried out if one monitors the FFT of the interference patterns.

We next demonstrate two concepts for force sensing.

III. ACCURATE FORCE SENSING

Our PCF interferometer was pressed with a flat and a serrated mechanical piece with two grooves ($L_p = 1$ mm) separated 7.5 mm) or into a V groove see Fig. 3. The reflection spectrum for each applied force was collected and the FFT was calculated.

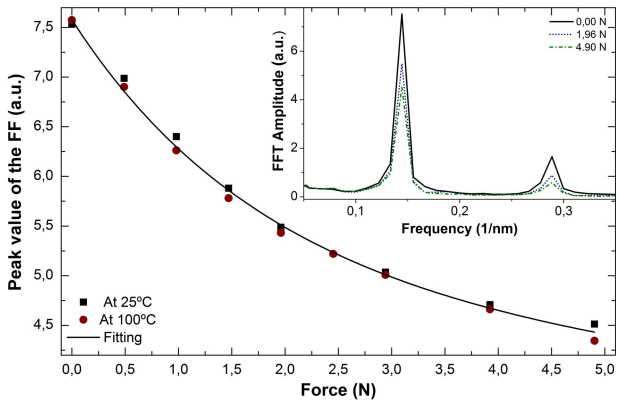


Fig. 5. Peak value of the FFT amplitude as a function of force observed in a 3.7 cm-long interferometer. The inset shows the FFT amplitude as a function of frequency at three different forces. The device was pressed with a plate with two grooves separated 7.5 mm and L_p was 1 mm.

Figure 5 shows the peak value of the fundamental frequency (FF) of the FFT as a function of force measured at different temperatures. The results shown in Fig. 5 were obtained with the configuration depicted in Fig. 3(a). The inset of Fig. 5 shows the FFT amplitude as a function of frequency. The fundamental frequency (the highest peak) is located at $1/P$, where P is the period of the interference pattern. It is interesting to note that the behavior of the device is not affected by temperature changes, at least in the 25–100 °C range. The reason of this behavior is due to the fact that temperature does not affect the intensity of the interfering modes, hence, the fringe contrast of the interference pattern, and consequently, the peak value of the FFT. We did not carry out measurements at higher temperatures because the polymer that protected our PCF cannot withstand elevated temperatures. However, it is possible to coat PCFs with polymers that have higher operating temperature range. Some acrylates, silicone, or polyimide, for example, can resist temperatures up to 150 or 400 °C [19]–[21], and gold coatings can withstand temperatures up to 800 °C [22]. The protecting coating of the PCF does not affect the interfering modes neither the fringe contrast of the interferometer. Thus, it seems feasible to tailor the operating temperature range of the PCF interferometers here proposed.

Due to the short segment of the PCF needed to build the interferometer, the influence of the number of grooves on the performance of the same could not be investigated. However, it is not difficult to see that a large number of grooves will increase the area of the PCF that is contact with the mechanical piece. Consequently, the stress and strain on the PCF will diminish and the shift or visibility changes of the interference pattern will be less prominent. Thus, pressing the interferometer with mechanical pieces with a large number of grooves will result in low force sensitivity.

In another experiment we pressed our interferometer with a plate with one groove ($L_p = 2$ mm) when the device was semi-embedded on a plate with a V-groove, see Fig. 3(b). Our results are summarized in Fig. 6. As expected the changes of peak value of the FF (~1.3 per N) are more prominent

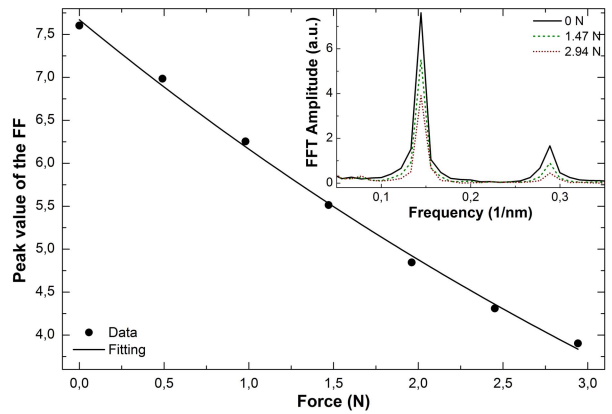


Fig. 6. Peak of the FFT amplitude as a function force on a 3.7 cm-long interferometer. The inset shows the FFT amplitude at different forces. The interferometer was compressed with a 2 mm-wide groove plate and other with a V groove.

because the stress on the PCF is higher as the external force is concentrated in a smaller area. If changes of 0.1 of the peak value of the FF can be detected, then our device is capable of resolving forces of 0.06 N. Higher force sensitivity and resolution can be achieved by reducing the value of L_p but a very narrow groove may cause permanent damage to the device.

The results shown in Figs. 5 and 6 demonstrate the versatility and flexibility of the sensing configuration here reported. They suggest that the measuring range and/or sensitivity of our device can be adjusted with the width of the grooves or with the number of grooves.

IV. CONCLUSIONS

A mode interferometer comprising a few centimeters of PCF fusion spliced at the distal end of a standard single mode fiber and pressed with a simple serrated mechanical piece was proposed for lateral force sensing. In our configuration the external force on the device introduces changes to the interference pattern which can be quantified by means of Fourier transformation. We believe that with minor modifications our device is suitable to sense other physical parameters that can be converted to lateral force (e.g. load, pressure, impact, etc.).

The main advantage of the configuration here proposed are: *i*) compactness; as only a few centimeters of PCF are necessary to fabricate the devices, *ii*) simplicity; since to monitor changes of the interference pattern a low-power LED and a low-resolution OSA are required, and *iii*) immunity to temperature and to noise induced by power variations of the optical source or attenuation in the optical fibers and/or connectors. We believe that all these advantages along with the versatility of the sensing architecture are attractive for the development of highly-functional fiber optic sensors.

REFERENCES

- [1] T. Guo *et al.*, “Temperature-insensitive fiber Bragg grating force sensor via a bandwidth modulation and optical-power detection technique,” *J. Lightw. Technol.*, vol. 24, no. 10, pp. 3797–3802, Oct. 2006.

- [2] G. P. Behrmann, J. Hidler, and M. S. Mirotznik, "Fiber optic micro sensor for the measurement of tendon forces," *BioMed. Eng. OnLine*, vol. 11, no. 2, p. 77, Oct. 2012.
- [3] A. A. G. Abushagur, N. Arsal, M. I. Reaz, A. Ashrif, and A. Bakar, "Advances in bio-tactile sensors for minimally invasive surgery using the fibre Bragg grating force sensor technique: A survey," *Sensors*, vol. 14, no. 4, pp. 6633–6665, Apr. 2014.
- [4] J. Ge, H. Feng, Y. Chen, Z. T. H. Tse, and M. P. Fok, "Spiral-structured fiber Bragg grating for contact force sensing through direct power measurement," *Opt. Exp.*, vol. 22, no. 9, pp. 10439–10445, May 2014.
- [5] B. Dong, D.-P. Zhou, L. Wei, W.-K. Liu, and J. W. Y. Lit, "Temperature- and phase-independent lateral force sensor based on a core-offset multimode fiber interferometer," *Opt. Exp.*, vol. 16, no. 23, pp. 19291–19296, Nov. 2008.
- [6] M. Karimi *et al.*, "Lateral force sensing system based on different photonic crystal fibres," *Sens. Actuators A, Phys.*, vol. 205, pp. 86–91, Jan. 2014.
- [7] J. Chen, J. Zhou, and X. Yuan, "M-Z interferometer constructed by two S-bend fibers for displacement and force measurements," *IEEE Photon. Technol. Lett.*, vol. 26, no. 8, pp. 837–840, Apr. 15, 2014.
- [8] L.-Y. Shao and J. Albert, "Lateral force sensor based on a core-offset tilted fiber Bragg grating," *Opt. Commun.*, vol. 284, no. 7, pp. 1855–1858, Apr. 2011.
- [9] R. Ahmadi, M. Packirisamy, and J. Dargahi, "High sensitive force sensing based on the optical fiber coupling loss," *J. Med. Devices*, vol. 7, no. 1, p. 011001, Feb. 2013.
- [10] B. Dong and E. J. Hao, "Temperature-insensitive and intensity-modulated embedded photonic-crystal-fiber modal-interferometer-based microdisplacement sensor," *J. Opt. Soc. Amer. B*, vol. 28, no. 10, pp. 2332–2336, Oct. 2011.
- [11] J. Villatoro, V. Finazzi, V. P. Minkovich, V. Pruneri, and G. Badenes, "Temperature-insensitive photonic crystal fiber interferometer for absolute strain sensing," *Appl. Phys. Lett.*, vol. 91, no. 9, p. 091109, Aug. 2007.
- [12] J. Villatoro, V. P. Minkovich, and J. Zubia, "Locally pressed photonic crystal fiber interferometer for multiparameter sensing," *Opt. Lett.*, vol. 39, no. 9, pp. 2580–2583, May 2014.
- [13] A. Sánchez, S. Orozco, A. V. Porta, and M. A. Ortiz, "Elasto-optical behavior model of a step-index fiber under localized pressure," *Mater. Chem. Phys.*, vol. 139, no. 1, pp. 176–180, Apr. 2013.
- [14] A. Bichler, S. Lecler, B. Serio, S. Fischer, and P. Pfeiffer, "Mode couplings and elasto-optic effects study in a proposed mechanical microperturbed multimode optical fiber sensor," *J. Opt. Soc. Amer. A*, vol. 29, no. 11, pp. 2386–2393, Nov. 2012.
- [15] V. P. Minkovich, A. V. Kir'yanov, A. B. Sotsky, and L. I. Sotskaya, "Large-mode-area holey fibers with a few air channels in cladding: Modeling and experimental investigation of the modal properties," *J. Opt. Soc. Amer. B*, vol. 21, no. 6, pp. 1161–1169, Jun. 2004.
- [16] K. S. Lau, T. L. Chan, and K. H. Wong, "Force measurement by visibility modulated fiber optic sensor," *Appl. Opt.*, vol. 38, no. 34 p. 7163, Dec. 1999.
- [17] Z. L. Ran, Y. J. Rao, W. J. Liu, X. Liao, and K. S. Chiang, "Laser-micromachined Fabry-Perot optical fiber tip sensor for high-resolution temperature-independent measurement of refractive index," *Opt. Exp.*, vol. 16, no. 3, pp. 2252–2263, Feb. 2008.
- [18] C. Gouveia, P. A. S. Jorge, J. M. Baptista, and O. Frazão, "Fabry-Pérot cavity based on a high-birefringent fiber Bragg grating for refractive index and temperature measurement," *IEEE Sensors J.*, vol. 12, no. 1, pp. 17–21, Jan. 2012.
- [19] K. Satori, K. Fukuchi, Y. Kurosawa, A. Hongo, and N. Takeda, "Polyimide-coated small-diameter optical fiber sensors for embedding in composite laminate structures," *Proc. SPIE*, vol. 4328, p. 285, Aug. 2001.
- [20] S. R. Schmid and A. F. Toussaint, "Optical fiber coatings," in *Specialty Optical Fibers Handbook*, A. Méndez and T. F. Morse, Eds. New York, NY, USA: Elsevier, 2007, pp. 95–122.
- [21] A. A. Stolov, D. A. Simoff, and J. Li, "Thermal stability of specialty optical fibers," *J. Lightw. Technol.*, vol. 26, no. 20, pp. 3443–3451, Oct. 15, 2008.
- [22] S. M. Popov *et al.*, "Optical loss of metal coated optical fibers at temperatures up to 800 °C," *Opt. Memory Neural Netw.*, vol. 21, no. 1, pp. 45–51, Mar. 2012.